# Active Site Ionicity and the Mechanism of Carbonic Anhydrase

**M. Krauss*,† and D. R. Garmer‡,§**

*Contribution from the National Institute of Standards and Technology, Gaithersburg, Maryland 20899, and Center for Advanced Research in Biotechnology, Maryland Biotechnology Institute, 9600 Gudelsky Drive, Rockville, Maryland 20850.*
*Received September 19, 1990*

**Abstract:** We report ab initio calculations on a cluster model for the active site of the enzyme carbonic anhydrase that considers the effect of the ionicity of the site on the energetics of ligand binding and reaction behavior. Hydrolysis occurs by a direct attack of the Zn-bound hydroxyl oxygen on the carbon atom of $CO_2$ with a small activation energy. The final product state in the cluster model has bicarbonate bound by one short and one long metal to oxygen bond. Detailed mechanisms for the initial attack of $OH^-$ on $CO_2$ and proton movement out to the free oxygen atom were studied by locating intermediates and transition states. Two mechanisms for rearrangement of bound bicarbonate to its most stable form are found to have low barriers. The first involves rocking of the bicarbonate from the initial intermediate. The second accomplishes this shift by a cyclic exchange of protons with a hydrogen-bound water or Thr-119. A Glu residue is hydrogen bonded to $N_{E2}$ of a tripod His in known carbonic anhydrase structures. Model calculations indicate the possibility of proton transfer to Glu simultaneous with the protonation of zinc-bound hydroxyl, which may explain observed NMR shifts of the histidine protons as a function of pH. Regardless of the proton position, the anionic residue qualitatively changes the electrostatic potentials in the active site region and the binding energies of other anionic ligands. The presence of the anionic residue is important in the release of product bicarbonate and also increases the exothermicity of the initial hydrolysis step. Binding of the $CO_2$ substrate is essentially unaffected by the presence of the anionic residue and also by the deprotonation of the metal-bound water, explaining the lack of any dependence on the pH of the Michaelis-Menten parameter $K_M$. Available coordination sites were examined for clusters of zinc and three ammonias with two waters, hydroxyl and water, or thiocyanate anion and water. The proton affinity of bound hydroxyl was unaffected by an increase in the zinc coordination number. In the presence of an anionic ligand, water is energetically favored as a second-shell ligand hydrogen-bound to the anionic ligand rather than as a fifth ligand bound to the Zn cation. The thiocyanate structure agrees well with experiment.

## Introduction

Carbonic anhydrase is a zinc metalloenzyme that catalyzes the reversible hydration of $CO_2$. The mechanism has been written[1] as

$$ZnOH^- + CO_2 \leftrightarrow ZnHCO_3^- \leftarrow (H_2O) \rightarrow ZnOH_2 + HCO_3^- \leftrightarrow ZnOH^- + H^+ + HCO_3^-$$

The hydration of $CO_2$ is dominant above pH 7, while the dehydration of the bicarbonate anion is observed below pH 7. The hydration of carbon dioxide is facilitated through an activated water or $ZnOH^-$ species.[2,3] The metal is considered to serve the function of reducing the deprotonation enthalpy of water.[4,5]

Merz et al.[6] have briefly outlined a widely accepted molecular mechanism[1,3,7] and presented the most detailed quantum chemical calculations of first-shell models to date. In the first step, the field of the cation assists the deprotonation of the water bound to zinc. $ZnOH^-$ then attacks the approaching $CO_2$ substrate to form the Zn-bicarbonate species. Product release is presumably obtained then by competitive binding with water or hydroxyl anion. There are a number of variants on this mechanism that differ on details regarding the possibility of four- or five-coordinate binding in the initial and final states, the extent to which the $CO_2$ is polarized by or bound to the Zn cation during reaction, the conformation of the transition state, and the mechanism and ease of intra- and intermolecular proton transfer. A feature of all the theoretical analyses is the assumption that the three histidine residues that form a tripod bound to the zinc cation are neutral. The ionicity of the first-shell metal complex at the active site is then +2 at low pH when one or two waters are bound to the zinc-tripod or +1 when hydroxyl is bound.

In this paper, we show that the ionicity of the active site metal complex is different than assumed in previous models. An examination of the crystal structures of a number of apparently dissimilar Zn enzymes has shown an intriguing similarity in the electronic structure at the active site. In many, if not all cases, there is a Glu or an Asp in the second shell hydrogen-bound to a first-shell histidine.[8,9] The Glu or Asp-His-zinc interacting triad has been found in at least 30 protein structures.[10] Since the histidine is bound to a doubly charged cation, the possibility of transferring the proton from the histidine to the aspartate or glutamate must be considered. This is more likely for CA than the Zn proteases since there is no other anionic residue in the first shell unless the water ligand is deprotonated. The proton has been predicted to stay with the histidine in the active site of carboxypeptidase[11] where the Zn cation is also directly coordinated to a Glu. The pattern of hydrogen bonds in the CA active site (isozyme II) has also been drawn to suggest the hydrogen is on the histidine.[12] In the case of CA, Glu-117 is hydrogen-bound to His-119. The other two His ligands of the Zn are hydrogen-bonded, His-96 by Asn-244 and His-94 by Gln-92, which may also stabilize the His protons but should not qualitatively affect the electrostatic potential. The possibility of ionizing a histidine in addition to the water has been suggested,[13,14] but NMR data

† National Institute of Standards and Technology.
‡ Maryland Biotechnology Institute.
§ Present address: Mt. Sinai Medical Center, Biophysics Department, New York, NY.

(1) Coleman, J. E. In *Zinc Enzymes*; Bertini, I., Luchinat, C., Maret, W., Zeppezauer, M., Eds.; Birkhauser: Boston, 1986; pp 49-58.
(2) Lindskog, S.; Coleman, J. E. *Proc. Natl. Acad. Sci. U.S.A.* **1973**, *70*, 2505.
(3) Silverman, D. N.; Lindskog, S. *Acc. Chem. Res.* **1988**, *21*, 30.
(4) Demoulin, D.; Pullman, A. *Theor. Chim. Acta* **1978**, *49*, 161.
(5) Pullman, A. *Ann. N.Y. Acad. Sci.* **1981**, *367*, 340.
(6) Merz, K. M.; Hoffmann, R.; Dewar, M. S. *J. Am. Chem. Soc.* **1989**, *111*, 5636.
(7) Liang, J.-Y.; Lipscomb, W. N. *Int. J. Quantum Chem.* **1989**, *36*, 299.
(8) Argos, P.; Garavito, R. M.; Eventhoff, W.; Rossmann, M. G.; Branden, C. I. *J. Mol. Biol.* **1978**, *126*, 141.
(9) Valee, B. L.; Auld, D. S. *Proc. Natl. Acad. Sci. U.S.A.* **1990**, *87*, 220.
(10) Christianson, D. W.; Alexander, R. S. *J. Am. Chem. Soc.* **1989**, *111*, 6412.
(11) Nakagawa, S.; Umeyama, H. *Chem. Phys. Lett.* **1981**, *81*, 503.
(12) Lindskog, S. See ref 1, pp 307-316.
(13) Bertini, I.; Luchinat, C.; Scozzafava, A. *Inorg. Chim. Acta* **1980**, *46*, 85.
(14) Appleton, D. W.; Sarkar, B. *Proc. Natl. Acad. Sci. U.S.A.* **1974**, *71*, 1686.

have been interpreted to reject the ionization of a histidine to an imidazolate anion.[15,16] However, neither of these conclusions considered the proton as shuttling between hydrogen-bonded atoms, so the position of the hydrogen-bonded proton in the His–Glu couple is still an open question that has not been considered as yet in the discussion of the CA mechanism. The formal ionicity of the active site metal complex is reduced by one with the presence of the Glu–His hydrogen-bonded couple. The electrostatic potential around the first-shell active site complex is then different from the potential that the earlier models predict, which will influence the effective proton affinities, the binding of the substrate or inhibitor, especially if it is anionic, the rate-determining proton-transfer step, the course of the transition-state vector, and the release of final product. All aspects of the mechanism that are driven by the enthalpic changes then have to be reconsidered as a function of the ionicity of the active site.

There have been several ab initio theoretical studies of the mechanism of carbonic anhydrase,[5,17,18] but none has examined the transition states of the various steps in the mechanism with ligands that have a full complement of valence electrons. A number of semiempirical studies examined both energetics and transition states but have differed in details with the ab initio studies.[6,7] Allen et al.[17] have examined the effect of local anionic fields but focused, as did Pullman,[5] on the Thr-119–Glu-106 hydrogen-bonded couple. None of these studies have considered the possibility of a first-shell anionic residue and the concomitant shuttling of a proton between the Glu and His residues.

We shall first examine the energetics of a model for the His–Glu couple. The presence of the anion at either His-119 or Glu-117 leads to electrostatic potentials at the active site qualitatively different from those that result from neutral first-shell models, and these potentials will be presented as a function of the ionicity of the complex. The presence of the anion also leads to very large shifts in the proton affinities of the hydroxyl anion that is bound to the metal cation. These shifts in the proton affinities are related to $pK_a$ shifts in ligands bound to metal cations, and the magnitudes of the shifts suggest that the protein would not be active around a pH of 7 without the first-shell anionic residue.

The binding of the ligands to a metal cation is primarily due to electrostatic forces, and the presence of an anion will have a substantial effect on such ligand binding energies.[19,20] The presence of hydrogen-bonded anionic residues in the second shell can have comparable effects to the those in the first shell. The putative hydrogen bonding of the Zn-bound water, hydroxyl anion, or product bicarbonate to a Thr-199 bound to Glu-106 has been given considerable attention.[3,5,17,18,21] Variations in the electrostatic potential map have been suggested to be the source of both large kinetic and effective $pK_a$ differences in the isozymes of CA.[3,22] Even a partial proton transfer between two residues could lead to substantial electrostatic potential differences at the active site and a large shift in the effective $pK_a$.

The hydration reaction is examined initially with the neutral tripod model, and then the influence of the His–Glu couple is considered. When the carbon dioxide substrate is allowed to approach $ZnOH^-$, three intermediate states are found for (a) unreacted $CO_2$ bound in the "second shell" as a Michaelis complex, (b) metal-bound bicarbonate anion with the hydrogen on the Zn-bound oxygen, and (c) the bicarbonate after intramolecular hydrogen transfer or rotation of the bicarbonate. The unreacted $CO_2$ can be considered to displace a "deep" or second-shell water that apparently is not bound directly to Zn but is in an array of nine crystallographically observed waters.[23] The energetics are determined with and without the presence of the anionic residue. This work repeats some of the earlier theoretical analyses since the effect of the anionic residue has to be examined in a consistent set of calculations considering a complete first shell of metal ligands.

In the initial deprotonation equilibrium and for product release, the question of the coordination number at the metal cation is important and will be examined with our model. The binding energy results as a function of ionicity suggest that the displacement of product bicarbonate anion requires the anion associated with the His–Glu couple. The structure of the clusters will be compared with experiment to support the structural accuracy of the calculations.

**Table I.** Properties of Optimized Complexes of $Zn^{2+}$ with One Ligand

| zinc basis | ligand | ligand basis | ligand binding (kcal) | proton affinity (kcal) | $r_{ZnX}$ (Å) | $a_{ZnXY}$ (deg) |
|---|---|---|---|---|---|---|
| small[a] | $OH^-$ | CEP-31G | 410.7 | 91.6 | 1.712 | 144.3 |
| large[b] | | CEP-31G | 419.3 | 90.7 | 1.720 | 142.7 |
| large | | CEP-31G*+ | 405.7 | 87.4 | 1.744 | 123.3 |
| small | $H_2O$ | CEP-31G | 93.5 | | 1.948 | 125.3[c] |
| large | | CEP-31G*+ | 90.4 | | 1.893 | 126.2[c] |
| small | $CO_2$ | CEP-31G | 73.7 | | 1.826 | 180.0 |
| large | | CEP-31G*+ | 66.4 | | 1.865 | 180.0 |
| small | $NCS^-$ | CEP-31G | 330.2 | | 1.720 | 180.0 |
| small | $SCN^-$ | CEP-31G | 325.2 | | 2.270 | 98.0 |
| large | | CEP-31G* | 335.6 | | 2.193 | 92.5 |
| small | $NCO^-$ | CEP-31G | 331.4 | | 1.709 | 180.0 |
| small | $OCN^-$ | CEP-31G | 321.5 | | 1.667 | 180.0 |

[a] Minimal (3/3) with 28-electron-core CEP. [b] (4121/4121/41) basis with 10-electron-core CEP of ref 46. [c] $Zn^{2+}OH_2$ complexes converged to $C_{2v}$ symmetry.

## Methods

The model systems in this work consist primarily of zinc complexes with imidazole (Im) or ammonia, water or hydroxyl, carbon dioxide, and formic acid ligands that mimic substrate and protein components. Most calculations use compact effective core effective potentials (CEP) derived by Stevens et al.[24] Two different core representations are used for the zinc dication. Geometry optimization runs utilized a 28-electron-core CEP with a minimal 3-GTO sp basis representing the 4sp shell.[25] At single points where noted, the 3spd electrons were removed from the core and a 10-electron-core CEP was used for valence-electron calculations.[26] Comparison of the 10- and 28-electron CEP calculations using CEP-31G ligands shows that they yield comparable structures, relative energetics, dipole moments, and interaction energy components.[25] As usual, small basis set binding energies tend to be overestimated because of the large calculated dipole moments of the ligand. This is illustrated by relevant comparisons in Table I for a single ligand where successively larger basis sets were introduced. We have found, as did Kitchen and Allen,[27] that adding polarization functions to a zinc-bound heavy atom sometimes decreased the ZnXY angle as illustrated for $Zn^{2+}OH^-$ in Table I. In the case of $Zn^{2+}OH^-(NH_3)_3$, the ZnOH atoms become nonlinear when a d shell is added to the oxygen regardless of which zinc basis is used. However, it was found that the energy dependence on the ZnOH angle was very slight in any basis, so the neglect of polarization functions on oxygen will not lead to significant structural errors.

The structural information is shown to be reasonably calculated even for small basis sets by comparison with a structure with a full first shell. The structure of $Zn^{2+}(OH_2)_6$ has been determined by neutron diffraction.[28] The small zinc basis/CEP-31G optimized Zn–O distance is 2.046 Å versus 2.032–2.133 Å from experiment, and $r_{OH}$ is 0.959 Å versus 0.961–0.978 Å.

(15) Campbell, I. D.; Lindskog, S.; White, A. I. *Biochim. Biophys. Acta* **1977**, *484*, 443.
(16) Bertini, I.; Canti, G.; Luchinat, C.; Mani, F. *J. Am. Chem. Soc.* **1981**, *103*, 7784.
(17) Cook, C. M.; Haydock, K.; Lee, R. H.; Allen, L. C. *J. Phys. Chem.* **1984**, *88*, 4875.
(18) Jacob, O.; Cardenas, R.; Tapia, O. *J. Am. Chem. Soc.* **1990**, *112*, 8692.
(19) Voityuk, A. A. *J. Mol. Struct.* **1990**, *205*, 113.
(20) Bertini, I.; Luchinat, C.; Rosi, M.; Sgamellotti, A.; Tarantelli, F. *Inorg. Chem.* **1990**, *29*, 1460.
(21) Kannan, K. K.; Petef, M.; Fridborg, K.; Cid-Dresdner, H.; Lovgren, S. *FEBS Lett.* **1977**, *73*, 115.
(22) Sheridan, R. P.; Allen, L. C. *J. Am. Chem. Soc.* **1981**, *103*, 1544.
(23) Eriksson, E. A.; Jones, T. A.; Liljas, A. See ref 1, pp 317–328.
(24) Stevens, W. J.; Basch, H.; Krauss, M. *J. Chem. Phys.* **1984**, *81*, 6026.
(25) Garmer, D. R. Private communication.
(26) Basch, H.; Stevens, W. J.; Krauss, M. To be published.
(27) Whitnall, J.; Kennard, C. H. L.; Nimmo, J.; Moore, F. H. *Cryst. Struct. Commun.* **1975**, *4*, 717.
(28) Kitchen, D. B.; Allen, L. C. *J. Phys. Chem.* **1989**, *93*, 7265.

**Table II.** Properties of Optimized Four-Coordinate Clusters

| cluster | ammonia basis | proton affinity | binding energy oxygen ligand[c] (kcal) | $r_{ZnO}$ (Å) |
|---|---|---|---|---|
| $Zn^{2+}OH^-(NH_3)_3$ | CEP-31G | 158.5 | 301.3 | 1.725[a] |
| $Zn^{2+}OH^-(NH_3)_3$ | STO-3G | 172.6 | 279.6 | 1.798[a] |
| $Zn^{2+}OH^-(NH_3)_2$(imidazole) | STO-3G | 182.5 | 268.8 | 1.771[b] |
| $Zn^{2+}OH^-(NH_3)_2$(imidazolate) | STO-3G | 253.1 | 190.5 | 1.815[b] |
| $Zn^{2+}OH_2(NH_3)_3$ | CEP-31G | | 50.9 | 1.962 |
| $Zn^{2+}OH_2(NH_3)_3$ | STO-3G | | 43.3 | 2.140 |
| $Zn^{2+}OH_2(NH_3)_2$(imidazole) | STO-3G | | 42.5 | 2.041 |
| $Zn^{2+}OH_2(NH_3)_2$(imidazolate) | STO-3G | | 34.8 | 2.047 |

[a] Linearity of the ZnOH atoms was found. [b] Near linearity of the ZnOH atoms. [c] With reference to fully optimized fragments.

**Table III.** Proton Affinities (kcal/mol) of Structures Derived from Crystal Coordinates or from Complete Optimizations (Given in Parentheses)[a]

| $Zn^{2+}(NH_3)_2OH^-$ | imidazole (His-119) | imidazolate (His-119) | formic acid (Glu-117) | formate (Glu-117) | proton affinity |
|---|---|---|---|---|---|
| X | X | | | | 181.3 (182.5) |
| X | | X | | | 252.8 (253.1) |
| X | X | | | X | 230.3 |
| X | X | | | R | 229.5 |
| X | | X | X | | 243.6 |
| X | | X | R | | 243.8 |

[a] An X signifies a quantum mechanical fragment included, while an R indicates that a fragment was modeled by an electrostatic potential and dipole polarizable points.

Ammonia ligands often have been substituted for imidazole ligands.[4] The similarity in structural and energetic results has been confirmed here for the CEP and concomitant basis sets. It was further found that reduction of the ammonia basis to the STO-3G type maintains the similarity of the structural and energetic properties of the water and hydroxyl ligands with those obtained by using CEP-31G imidazoles. This suggests that the electronic structure at the zinc is not substantially altered by ammonia ligands for imidazole. Evidence supporting this useful substitution is given in Table II from optimizations using the small zinc basis.

All calculations utilized the GAMESS system of codes.[29] Complete optimizations of the complexes and the reaction transition states were done with the small basis sets. Both four- and five-coordinate first-shell complexes are considered. The model clusters used for specific problem areas are described in the section on results for the initial reactants, the transition states, the products, and an experimentally observed inhibitor, $NCS^-$.[30] Comparisons of the intrinsic energetics of five-coordinate structures with the binding of a ligand to the second shell of a four-coordinate complex will provide insight into the equilibrium structures at the active site and the process of proton transfer and relaxation. The effect of the His–Glu H-bonded couple is explored with both an all-valence-electron calculation including the second-shell formic acid representation of the Glu residue and a reaction field[31] version of the second-shell Glu.

## Results and Discussion

**His–Glu Couple: Where is the Proton?** The first shell of $Zn^{2+}$ was chosen as two ammonias and one imidazole to represent the His tripod and either a water or hydroxyl anion as the fourth ligand. A carboxylate anion (Glu-117) was initially hydrogen bound to the H(N) of imidazole (His-119). The imidazole and carboxylate coordinates were chosen from experimental isozyme II coordinates[32] with hydrogens added by QUANTA.[33] The other ligand coordinates are obtained from CEP-31G optimizations on $ZnX(NH_3)_3$ complexes, with X being water or hydroxyl. A resulting structure is shown in Figure 1.

The energetics of transferring the proton along the N–O line in the small basis are represented in Figure 2. Imidazolate is found as the stable form in the presence of both $H_2O$ and $OH^-$. With $H_2O$ present, formic acid is preferred by 16 kcal and only a shoulder is found in the energy curve to suggest the attraction

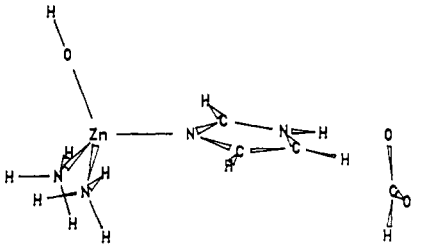

Figure 1. A protein fragment used to study His–Glu proton transfer.

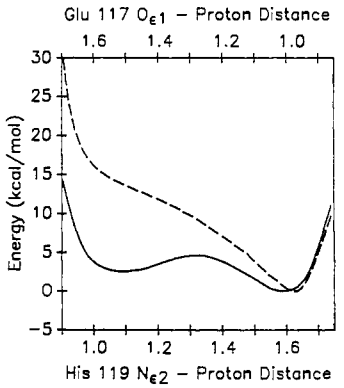


Figure 2. Energy curves for His–Glu proton transfer with bound hydroxyl anion (solid line) or water (dashed line).

to imidazole. However, the first-shell $OH^-$ reduces the exothermicity of proton transfer to 2 kcal. A double well energy curve is found with a small barrier of 5 kcal for moving the proton from formic acid to imidazolate. Double minimum for similar proton transfers in the presence of metal cations have been predicted.[34]

It is interesting to know whether direct quantum mechanical effects of the proton transfer are important in determining cluster properties. Examination of the gross populations along the proton-transfer energy curve determines only small shifts at the N···H···O atoms and very small changes elsewhere. Whether even small shifts can have an effect was tested by representing the formic acid or formate in the second shell with an effective fragment potential.[31] The effective fragment potential (EFP) consists of an electrostatic potential and a distributed polarizability so that the species can both influence the electronic structure of

(29) Schmidt, M. W.; Boatz, J. A.; Baldridge, K. K.; Koseki, S.; Gordon, M. S.; Elbert, S. T.; Lam, B. GAMESS. *QCPE Bull.* **1987**, *7*, 115.
(30) Eriksson, A. E.; Jones, T. A.; Liljas, A. *Proteins* **1988**, *4*, 274. Eriksson, A. E.; Kylsten, P. M.; Jones, T. A.; Liljas, A. *Proteins* **1988**, *4*, 283.
(31) Garmer, D. R.; Stevens, W. S.; Krauss, M.; Basch, H. To be published.
(32) Kannan, K. K.; Ramanadham, M.; Jones, T. A. *Ann. N.Y. Acad. Sci.* **1984**, *429*, 49. Structure 2CAB in Protein Data Bank, Brookhaven National Lab.
(33) QUANTA 2.0; Polygen Corp.: Waltham, MA, 1988.
(34) Basch, H.; Krauss, M.; Stevens, W. J. *J. Am. Chem. Soc.* **1985**, *107*, 7267.

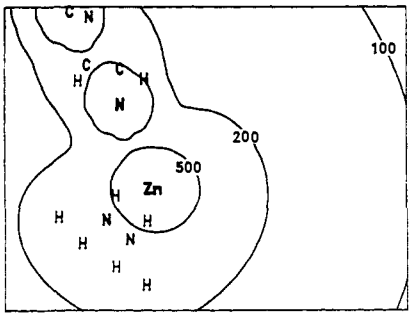


**Figure 3.** Electrostatic potential slice for a $Zn^{2+}(NH_3)_2$(imidazole) tripod. Values are given in kilocalories per mole.

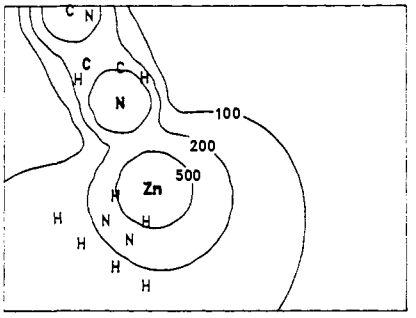


**Figure 4.** Electrostatic potential slice for a $Zn^{2+}(NH_3)_2$(imidazolate) tripod.

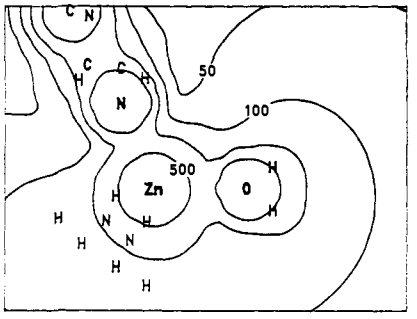


**Figure 5.** Electrostatic potential slice for a $Zn^{2+}OH_2(NH_3)_2$(imidazolate) cluster.

the zinc cluster and respond to the electrostatic field of the cluster. As seen in Table III, the EFP second-shell effects on the cluster proton affinity are in almost perfect agreement with the use of all-valence-electron calculation including the second shell. This suggests that the proton transfer shifts the centroid of the charge distribution without much accompanying electronic screening from electronic density movement between the species.

**Electrostatic Potential of the Initial Active Site.** Electrostatic potentials of the active site are qualitatively affected by the presence of an anion in the first shell or hydrogen-bonded to the second shell. The sign of the potential in the region of approach of the substrate is changed by the presence of the anionic residue. Representative potentials at the active site have been generated for possible ionic models of the initial protein state. The zinc–tripod complex is represented by $Zn^{2+}(NH_3)_2Im$ and $Zn^{2+}(NH_3)_2Im^-$. Since both complexes are positively charged, only positive potentials are found in Figures 3 and 4 that are roughly spherical around Zn as observed earlier.[35] The tripod has little qualitative effect on the character of the potentials that point toward the unoccupied ligand position. Addition of the water to the second complex again leads to potentials in Figure 5 that are all positive and roughly spherical around both the zinc and the water ligand. Weak negative potentials are first observed in Figure 6 off the oxygen of the hydroxyl anion bound to the +2 tripod. When there are two anionic groups and overall electrical neutrality,

(35) Osman, R.; Weinstein, H. *Isr. J. Chem.* **1980**, *19*, 149.

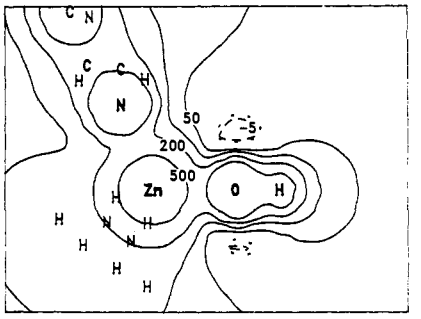


**Figure 6.** Electrostatic potential slice for a $Zn^{2+}OH^-(NH_3)_2$(imidazole) cluster.

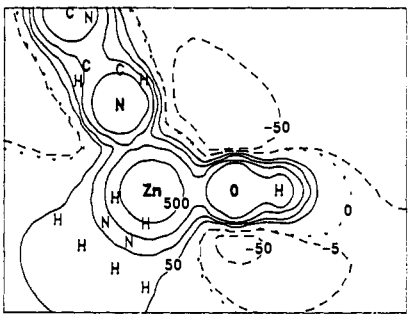


**Figure 7.** Electrostatic potential slice for a $Zn^{2+}OH^-(NH_3)_2$(imidazole) cluster.

large negative regions appear to provide sites for attack at the oxygen as shown in Figure 7. The effect of other residues that line the active site can also be substantial, but for isozyme II they are not charged, or as in the case of the partially buried Glu-106 or the catalytically important His-64, screened by the waters or hydrogen-bonded residues from the first-shell region.

**Proton Affinities.** The calculated proton affinity (PA) of $OH^-$ is greater than $Im^-$ in vacuo and in solution, but in the presence of the Zn dication the relative values are reversed as the proton affinities are greatly reduced.[5,6] Oxygen proton affinities in the first-shell model based on the protein structure are summarized in Table III. Proton affinities of the hydroxyl and imidazolate anions in completely optimized structures agree well with the model values. In a $Zn^{2+}(NH_3)_3Im^-OH^-$ system, the proton affinity of $OH^-$ is reduced to 253 kcal/mol from a calculated value of 409 kcal/mol for the gas-phase anion and for imidazolate the PA is reduced to 273 from 370 kcal/mol. The proton affinity of the hydroxyl decreases to 181 if the imidazolate is protonated and for the imidazolate decreases to 201 kcal/mol if the hydroxyl is protonated. The large proton affinity variation with ionicity of the first-shell complex is, of course, determined by the large variation in the ionic bond energy of hydroxyl or imidazolate anions. As can be seen in Table II, the reduction in the neutral $H_2O$ bond energy is only 10% of that for $OH^-$ and is smaller as a percentage of bond energy.

A model of Glu-117 is now added to the second shell. A formic acid hydrogen-bonded to the imidazolate shifts its PA slightly to 244 kcal/mol, while the proton transfer to the imidazolate results in another reduction to 230 kcal/mol. Since this is still a shift of 49 kcal/mol from the results without an anion in the model, it is apparent that the anionic character has a primary effect of changing the energies of the end points of the water deprotonation step in the CA mechanism. The position of the proton between His-119 and Glu-117 is of lesser importance, resulting in a difference of only 13 kcal/mol. A calculation of the PA for $SH^-$ or $Im^-$ in a zinc-finger model[24] also finds a shift of about 70 kcal/mol as a function of ionicity. The presence of the anionic potential in or near the first shell has a comparable effect on the PA of two very different anions. Cook et al.[17] also concluded that the effective proton affinity will shift by 70 kcal/mol per unit charge change in the electrostatic potential. Their model studies concluded that the ZnOH proton affinity would be 220 kcal/mol but in the presence of the Glu–Thr couple, which is probably more

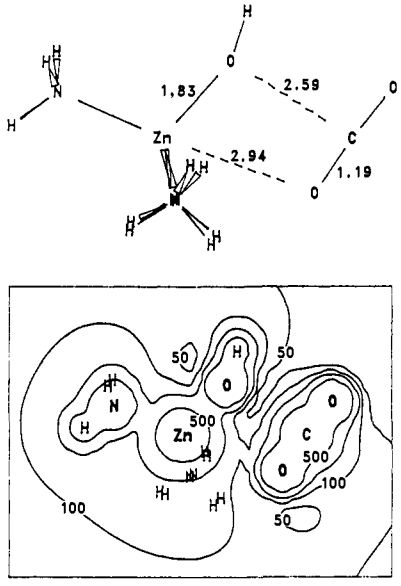


Figure 8. (a) Optimal structure O1 and (b) electrostatic potential.

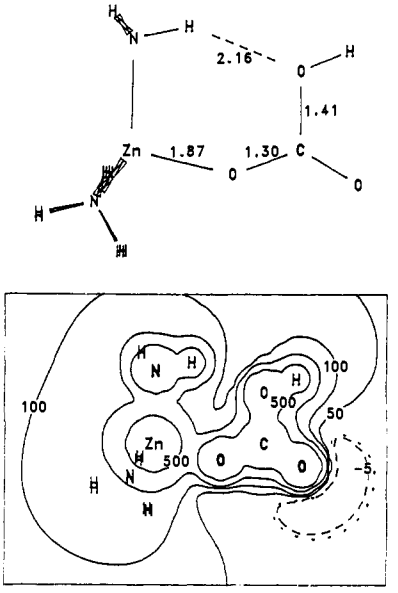


Figure 9. (a) Optimal structure O2 and (b) electrostatic potential.

shielded from the metal site. Without consideration of the extended networks of hydrogen bonds that are associated with both the His–Glu and Thr–Glu couples, it is impossible to predict the additivity of the effect of these ionic residues on the PA but it is evident that large shifts in the proton affinity are expected from the presence of charged residues in the first or second shell of the metal complex.

**Reactive Pathways.** The negative electrostatic potentials near the oxygen in the ZnOH models (Figures 6 and 7) provide an approach to attack the $CO_2$. In this section, we shall address two questions that have been raised about the energy surface for the reaction complex by all theoretical calculations. First, does the $CO_2$ approach the metal and bind an oxygen in the transition state? Another way of asking the question is whether the transition state is a simple attack of O(H) to the C atom or if there is a four-center interaction with the Zn cation polarizing the oxygen on the $CO_2$. Second, is the nucleophilicity of the OH reduced by being bound to the cation sufficiently to introduce a substantial activation energy? These questions were addressed by Pocker and Deits[36] in one of the first kinetic studies to provide strong evidence for the ZnOH moiety as controlling the activity. We will then consider how the answers are modified by the presence of an anionic residue in the first shell of the metal complex.

Three stationary points have been obtained of intermediates representing (a) nonreactive binding of $CO_2$ as in Figure 8 (labeled O1), (b) partially bidentate binding of the bicarbonate as in Figure 9 (labeled O2), and (c) another partially bidentate bound bicarbonate with the short metal to oxygen bond rotated as in Figure 10 (labeled O3). The hydrogen atom remains on the initial hydroxyl oxygen, and the product bicarbonate rotates the metal to oxygen bonds to lower the energy. Gradient-optimized structures were obtained with three STO-3G ammonias for the tripod but the relative energetics tested by substituting a CEP-31G imidazole or imidazolate for an ammonia. The transition states separating these structures have also been located. Hessians were calculated for all five structures, verifying their nature. The transition states were followed to the nearest optima in standard optimization runs, rather than in an intrinsic reaction coordinate run. Therefore, there could be intermediate stationary points of secondary importance that are bypassed and not found. Certain other stationary points had the plane of the reactive species rotated 30° relative to the tripod axis. It appeared that each was at higher energy than a corresponding nonrotated structure, and so none were further characterized.

Nonreactive binding at O1 occurs for a O(ZnOH) to C distance of 2.59 Å. $CO_2$ remains almost linear with a bending angle of

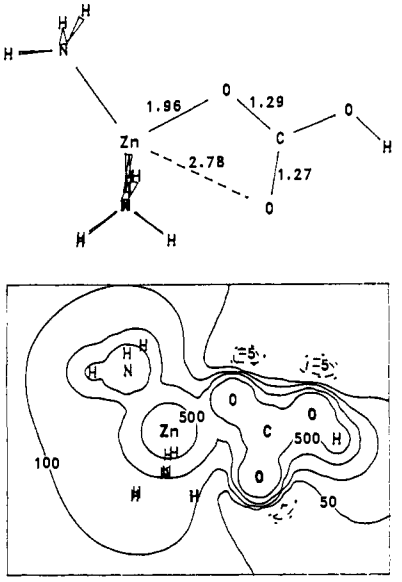


Figure 10. (a) Optimal structure O3 and (b) electrostatic potential.

175° and the C–O bond length distortions are of 0.01 Å. The vibrational frequency of the asymmetric stretch of $CO_2$ is shifted by only a few inverse centimeters as is observed,[37] but this is nonetheless a productive mode of binding. The Mulliken population suggests some polarization, with the O(C) closest to the Zn having an atomic charge of –0.25 compared to –0.08 for the O furthest from Zn. However, the Zn–O distance is 2.94 Å, suggesting only a weak electrostatic binding. The binding energy is 11.7 kcal in the optimization basis, which includes a large basis set superposition error contribution. As the basis set is enlarged and improved, the binding energy is reduced to about 8 kcal/mol, increasing to 10 kcal with the MP2 correlation correction. From the orientation of the hydroxyl and carbon dioxide (see Figure 8a), it is likely that the binding energy comes from favorable interaction of the hydroxyl with the $CO_2$ carbon and from electrostatic interaction of the closest $CO_2$ oxygen with the dication field. Similar conclusions on $CO_2$ binding have been reached by Pullman[5] and Lipscomb.[7] However, the AM1 energy surface emphasizes H(Im) bonds to $CO_2$.[6] In optimizing a $ZnOH^-(NH_3)_2$(imidazole) cluster, a second optimum point with a 5 kcal/mol lower energy was found in addition to the one where

(36) Pocker, Y.; Deits, T. L. *J. Am. Chem. Soc.* **1981**, *103*, 3949.

(37) Riepe, M. E.; Wang, J. H. *J. Biol. Chem.* **1968**, *243*, 2779.

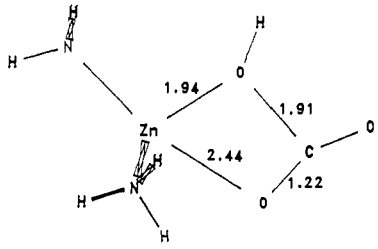


**Figure 11.** Transition-state structure T1.

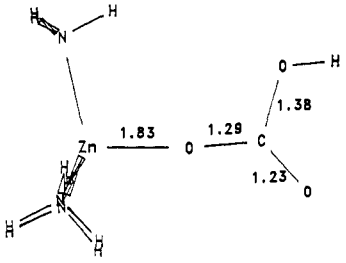


**Figure 12.** Transition-state structure T2.

the hydroxyl is in an apical position. This second optimum had a close contact of 2.45 Å between the hydroxyl oxygen and H(C2) of the imidazole. This structure is qualitatively similar to structure **3** of ref 6. Such internal hydrogen bonding is a common feature of attempts to model ionic sites with small clusters.[38] This internal hydrogen bond is not as strong as an internal ionic bond to water or with the $CO_2$ substrate, but is substantial enough to influence the structure of the total complex. The orientation of the imidazole planes in crystal structures also appears to be constrained by the nitrogen H bonds to values at least 30° away from the best H(C) contacts with fourth ligands.

In order to assess the affect of the anionic residue on the $CO_2$ binding energy, it is necessary to explicitly include the imidazole ligand by replacing one of the ammonias. Gradient optimization with these ligands was too expensive, and so we adopted the following modeling procedure. Each STO-3G ammonia was replaced in turn by a CEP-31G imidazole or an imidazolate, retaining the optimized coordinates of all other atoms and the zinc-bound nitrogen. Imidazole internal coordinates and orientation relative to the tripod were taken from His-119 in the crystal structure. The lowest energy structure from the three possible replacements was retained for the energetic comparisons. In this way, any close contacts that would invalidate comparisons are eliminated. Binding of $CO_2$ with the imidazole-substituted complex is 10.8 kcal/mol and increases to 12.4 kcal/mol for imidazolate. This suggests that, for a second-shell neutral ligand, binding to the zinc complex is determined primarily by the local interaction at short distances and not the ionicity of the first-shell metal complex.

The transition state T1 connecting O1 and O2 has only a 3.3-kcal forward barrier with the basis set used for optimization. The structure (Figure 11) appears to be closer to O1 than to O2, as would be predicted from the exothermicity of the step. The transition state T2 connecting O2 and O3 indicates a rocking mechanism for moving the proton out to the free oxygen. The forward barrier in this case is only 1.1 kcal. This transition state also appears to be closer to the reactant-side structure. However, the surface for rocking was found to be extremely flat over a wide range of Zn–O–C angles.

Local optima O2 and O3 both have one close ZnO contact and one longer contact. Like structure O1, the $CO_3H^-$ moiety is planar. The Zn–O distances in O2 are 1.87 and 3.36 Å, while in O3 they are 1.96 and 2.78 Å as seen in Figures 9a and 10a. O3 is obtained from O2 by in-plane rocking motion of the bicarbonate anion. Clearly there is little bidentate binding in both stationary points but considerable electrostatic or internal hydrogen bonding. Evidence of weak bidentate character is that the closest Zn–O contact distance is shorter in the unidentate rocking transition state T2 (Figure 12) than in O2 and O3. However, O2 is likely a local optimum because of the additional favorable electrostatic contact between the protonated oxygen and an ammonia proton of 2.16 Å. There is no need to break a chemical bond in moving the bicarbonate proton to the favorable energy position away from the metal cation. This sequence of structures are similar to those constructed by Jacob et al.[18] and all are substantially bound relative to the reactants. These results provide another mechanism for intramolecular proton transfer in addition to a water-assisted transfer of a proton from one oxygen atom to another.[7]

An informative decomposition is to separate the bicarbonate moiety ($CO_3H^-$) from all three stationary points, giving energetics summarized in Table IV. During the reaction, the binding energy of the moiety decreases because a strong Zn–O(H) bond is replaced by a weaker Zn–O(C) bond. This is more than compensated by the internal binding energy in the bicarbonate. The final step is made favorably by the rocking movement of the proton away from the dication.

An ammonia also has been replaced by imidazole or imidazolate for intermediates O2 and O3, yielding the energetics illustrated in Figure 13. For the replacement by imidazole, the overall stabilization in forming the O–C bond changes only slightly from 11.0 to 11.7 kcal/mol. The imidazolate, on the other hand, yields a stabilization of 17.2 kcal/mol through bond formation. This is due to a lesser destabilization of bicarbonate anion binding to Zn than for the $OH^-$ of O1. The energy change in accomplishing the outward proton movement yielding O3 is less affected by the introduction of an imidazole or the charged imidazolate ligand.

In Table V, we recalculated the stationary point energies at the MP2 level with polarization functions on the $CO_3H^-$ moiety and using the large zinc basis. The most significant changes from the small basis results are a decrease of 7.7 kcal in the exothermicity of the postulated first step from O1 to O2 and an increase in the barrier from O2 to O3 by 4.8 kcal. There is now a positive activation energy also for T2 relative to the Michaelis complex,

**Table IV.** Decomposition of $Zn^{2+}(NH_3)_3CO_3H^-$ Energetics (kcal/mol) Relative to O1

| stationary point | $Zn^{2+}(NH_3)_3$ internal energy | $CO_3H^-$ moiety internal energy | $Zn^{2+}(NH_3)_3$·$CO_3H^-$ interaction | total energy |
|---|---|---|---|---|
| O1 | 0 | 0 | 0 | 0 |
| O2 | −5.4 | −49.6 | 44.0 | −11.0 |
| O3 | −4.4 | −46.7 | 35.7 | −15.4 |

**Table V.** Relative Energies (kcal/mol) of the Stationary Points from Different Methods

| structure | HF/ optimization (small) basis | HF/ large basis | MP2/ large basis |
|---|---|---|---|
| O1 | 0 | 0 | 0 |
| T1 | 3.3 | 7.0 | 3.9 |
| O2 | −11.0 | −7.7 | −3.3 |
| T2 | −9.9 | −3.9 | 2.6 |
| O3 | −15.4 | −18.9 | −12.9 |

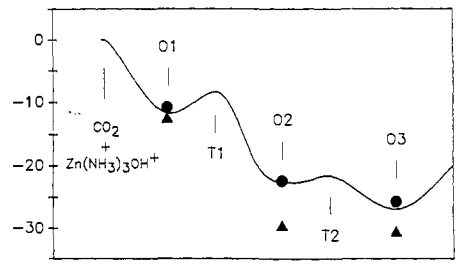


**Figure 13.** Energy profile for the model reaction sequence. Filled circles indicate energies with a tripod ammonia replaced by imidazole, and triangles indicate a substitution of imidazolate.

(38) Basch, H.; Krauss, M.; Stevens, W. J.; Cohen, D. *Inorg. Chem.* **1985**, *24*, 3313.

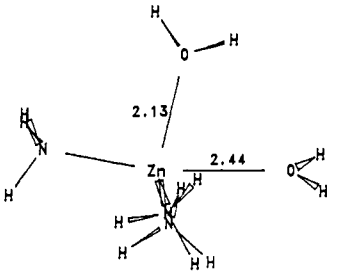


Figure 14. Optimal structure of $Zn^{2+}(OH_2)_2(NH_3)_3$ cluster.

O1. Significant overall reaction exothermicity is still apparent, and the qualitative behavior of the curve does not change. Figure 13 represents the small basis SCF results since the extent to which ammonia is still a good mimic for imidazole for the large basis or MP2 calculation has not been determined.

Liang and Lipscomb[7] postulate that the proton transfer from structure O2 to O3 can occur through a concerted proton exchange with a water molecule or Thr-199. PRDDO calculations indicated that a 3.5-kcal barrier existed for this process using one water molecule in the proton-transfer chain and a 1.4-kcal barrier with two water molecules in the chain.[7] The direct proton shift was found to have a much too large barrier.[7] We were able to stabilize a structure from O2 having the bicarbonate intact without ammonias by binding a water molecule in the position that would assist the proton transfer. Then a transition state was located 5.8 kcal above this connecting to a final state 1.3 kcal below the reactants. Both protons in the transfer chain were located approximately 0.4 Å closer to the water oxygen in the transition state. This is probably due to a significant extra binding of a carbonate dianion to $Zn^{2+}$ compared with the bicarbonate in the end point structures. The existence of a transition state with these characteristics probably rules out a local optimum with $H_3O^+$ bound to carbonate on this surface. The final state is true bidentate (Zn–O distances of 1.89 and 1.90 Å) with a water molecule hydrogen-bound to the bicarbonate proton. This confirms the PRDDO result, and it is unlikely that the energetics would change much with the tripod included since we have already shown that the reactant and product states would be of comparable energies.

Electrostatic potentials for the optimized structures in a model reactive pathway are given in Figures 8, 9, and 10. They show negative regions opposite to the tripod only after carbon dioxide has been incorporated by a chemical bond. The final and lowest energy structure has potential regions of roughly equal depth around all three oxygens. The negative charge initially concentrated on the hydroxyl anion is not entirely polarized to the oxygens in direct contact with the dication. It is distributed sufficiently to the exposed oxygens to give a potential reminiscent of neutral carbonic acid.

**Coordination Numbers.** Clusters for a $Zn^{2+}(NH_3)_3$ tripod (STO-3G ammonias) with two bound species that correspond to models of the initial reactants, final products, and an anionic inhibitor were explored for the relative energetics of first- and second-shell binding in five-coordinate structures. The optimizations were performed with initial guesses of intentionally distorted trigonal-bipyramidal or square-pyramidal structures to try to avoid the location of symmetrical saddle points. Two waters settled into nonequivalent first-shell positions with $r_{ZnO}$ of 2.13 and 2.44 Å as illustrated in Figure 14. The longer water bond is in the axial position of a distorted trigonal bipyramid, while the inner water is in an equatorial slot. The Zn–N distances are increased by approximately 0.05 Å from the $Zn^{2+}OH_2(NH_3)_3$ results. The binding energy of the second water molecule is calculated as 23.7 kcal, indicative of a comfortable accommodation. We have located the optimum structure of this type also using CEP-31G ammonias. The zinc–oxygen distances for this were 2.01 and 2.17 Å, suggesting that the use of STO-3G ammonias slightly favors lower coordination numbers. However, the binding energy of the second water is unchanged at 23.2 kcal. An optimization with two bound hydroxyls ejected an ammonia into a second-shell position.

Table VI. Species Binding Properties to Clusters in the Optimization Basis[a]

| bound species | cluster | BE (kcal) | $r_{ZnX}$[b] (Å) |
|---|---|---|---|
| $O_2COH^-$ | $Zn^{2+}(NH_3)_3$ | 233.4 | 1.956 |
| $NCS^-$ | | 208.8 | 1.899 |
| first-shell $H_2O$ | $Zn^{2+}(NH_3)_3OH_2$ | 23.7 | 2.436 |
| first-shell $CO_2$ | | 6.8 | 2.124 |
| second-shell $CO_2$ | | 12.0 | 3.268 |
| first-shell $H_2O$ | $Zn^{2+}(NH_3)_3OH^-$ | 13.8 | 2.172 |
| second-shell $H_2O$ | | 23.4 | 3.018 |
| first-shell $O_2COH^-$ | | 104.7 | 2.137 |
| first-shell $H_2O$ | $Zn^{2+}(NH_3)_3NCS^-$ | 12.5 | 2.148 |
| second-shell $H_2O$ | | 19.8 | 3.308 |
| first-shell $H_2O$ | $Zn^{2+}(NH_3)_3OCOOH^-$ | 19.8 | 2.103 |
| second-shell $H_2O$ | | 24.6 | 3.316 |

[a] See also Table II. [b] X is the closet heavy atom in the bound species.

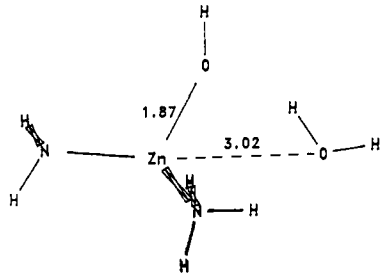


Figure 15. Optimal four-coordinate $Zn^{2+}OH^-(NH_3)_3\cdots OH_2$ cluster.

With a first-shell hydroxyl, a water may also weakly bind in the first shell or be ejected into a more strongly bound second-shell position (see Table VI and Figure 15). Hessians were calculated for these structures, verifying that both are local minima. In the latter structure, the hydroxyl and ammonia triads are only slightly distorted from the four-coordinate structure without water. The water orients to make close contacts with ammonia protons and to have one proton directed toward the hydroxyl. The Zn–O(OH) distance is increased by 0.08 Å to 1.87 Å due to this H bond. The interaction of the hydroxyl proton with the second-shell water also yields a bent O–H orientation with respect to zinc. Recent high-resolution crystal structures have indicated four-coordinate binding with probable bound hydroxyl.[30] The zinc–hydroxyl distances agrees with the corresponding ab initio structure to within 0.2 Å. The remaining error can be attributed to the still neglected hydrogen bonding to the second shell. From the energies for this structure and that with two bound waters, a decrease of only 1.0 kcal in the proton affinity is predicted due to the additional water molecule in the second shell.

The less stable five-coordinate structure also had one of the water O–H bonds oriented so as to make a partial favorable contact with the hydroxyl oxygen. This could also be considered as a distortion to make an O–H bond dipole favorably oriented with a $Zn^{2+}$–$OH^-$ dipole. A Zn–O–H angle of 81.7° resulted, whereas ~125° was found for most other water ligands. The hydroxyl was more strongly perturbed, with the Zn–O(OH) distance increasing by 0.18 Å to 1.98 Å. The more stable structure in which water ejected to the second shell appeared to do so with the water molecule coming from an axial position in a trigonal bipyramid, while the five-coordinate structure has the hydroxyl in this position and equatorial water. Therefore, we postulate that species bound to a complex by less than 20 kcal/mol must be in an equatorial site in order to produce a five-coordinate local minimum. Another postulate from this structural series which has not been directly tested is that for true five-coordinate structures, the lowest energy configuration will have the strongest binding ligands in equatorial positions.

The transition state for transferring a proton between two zinc-bound hydroxyls was located within the ammonia cluster model. The energy for this structure (having $C_S$ symmetry) was 2.6 kcal above the five-coordinate end points. This barrier is greater than for transferring a proton between a gas-phase hy-

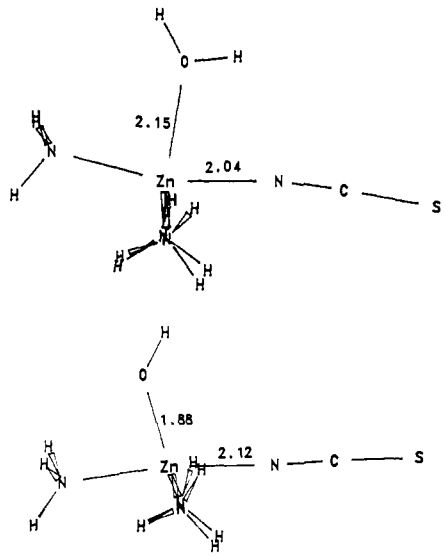


**Figure 16.** (a) Optimal five-coordinate $Zn^{2+}NCS^{-}OH_2(NH_3)_3$ cluster; (b) optimal five-coordinate $Zn^{2+}NCS^{-}OH^{-}(NH_3)_3$ cluster.

droxyl anion and a water, which is essentially zero, due to the presence of the zinc cation. An exploration of the complete energy surface for water or proton exchange will be complex and was not considered at this time.

Similar five- and four-coordinate structures and binding energies have been found for $Zn^{2+}(NH_3)_3NCS^{-}OH_2$, giving slightly weaker water binding in the first and second shells than for the hydroxyl in each case. Second-shell water binding also is energetically preferred in this case. The tripod structural parameters are very close to those of the hydroxyl structures. The five-coordinate structure shown in Figure 16a has one water O–H bond positioned to make a favorable contact with the anion, resulting in a Zn–O–H angle of 105.4°. Two anions, OH and NCS, are also bound in a comparable five-coordinate complex as seen in Figure 16b. The high-resolution crystal structures indicate five-coordinate binding with probable bound thiocyanate and water.[30] The zinc–water experimental distance agrees with the corresponding ab initio structure to within 0.1 Å and the O–Zn–N angle to within 10°, with the experimental angle being less than 90° diagnostic of bound water rather than hydroxyl. The calculated energetic similarities between thiocyanate and hydroxyl clusters would indicate that subtle environmental effects arising from the slightly different packing and electrostatic potentials are determining the observed coordination numbers for these particular bound anions.

Second-shell binding of carbon dioxide to four-coordinate clusters is similar in energy whether or not the water is ionized. This is in accord with the observation of no pH dependence for the $K_m$ binding constant.[3] $CO_2$ would appear to enter the first shell more easily with hydroxyl present rather than water(s) because of the exothermic reaction and the lack of a need to displace a possibly strongly bound water. However, competition between water and carbon dioxide for first- and second-shell sites would also be driven by the larger solvation energy of water, which might lead to a population of sites in which $CO_2$ had displaced bound water. The energy required to remove the proton from $Zn^{2+}(NH_3)_3OH_2OCO$ with $CO_2$ in the first shell is calculated to be 20 kcal less than for the five-coordinate complex with two waters. With $CO_2$ in the first shell and no internal water H bonding, removal of a proton should be very favorable and lead to reaction and bound bicarbonate eventually as structure O3.

Bicarbonate product is presumed to be driven off by the binding of the hydroxyl anion. The energetics of this mechanism were explored as well as the alternative of ejecting the neutral carbonic acid. We determined a minimum structure for bound water and bicarbonate as illustrated in Figure 17 and a structure with bound bicarbonate having a water in the second shell. The five-coordinate structure has significantly stronger water binding than was found with the other anions, which favors the idea that coordination

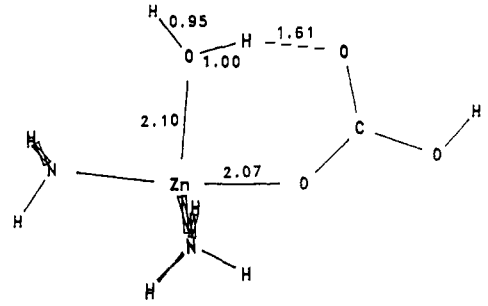


**Figure 17.** Probable globally optimal five-coordinate $Zn^{2+}OCOOH^{-}OH_2(NH_3)_3$ cluster.

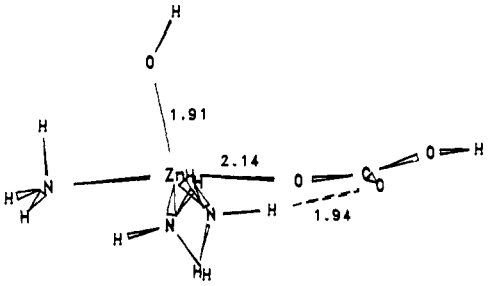


**Figure 18.** Optimal five-coordinate $Zn^{2+}OH^{-}OCOOH^{-}(NH_3)_3$ cluster.

number increases during the hydrolysis reaction. The bicarbonate is forced into a monodentate binding mode by the first-shell water, which agrees with the experimental distances found in a $^{13}C$ NMR study.[39] The bicarbonate is bound to this structure by 210 kcal. Proton removal from the water as a means of weakening the bicarbonate binding requires 278 kcal of energy. This is about 100 kcal greater than the requirement for removing a proton with only waters present and points out the need for intervention from the protein as screening or specific solvation if the leaving group from the first shell is to be bicarbonate.

The optimized five-coordinate complex with bound hydroxyl and bicarbonate is shown in Figure 18. The bicarbonate is unidentate but still very strongly bound, only 46 kcal less so than the hydroxide anion binding of 151 kcal to this complex. Upon replacement of one of the ammonias by imidazole in the manner described above, the binding of the bicarbonate decreases from 105 to 98 kcal, but replacement by imidazolate leaves only 19 kcal of binding energy. Such weak binding would assist in the removal of the product as bicarbonate.

Another possibility is for the leaving group to be neutral carbonic acid obtained by a proton transfer from bound water. This was examined by reoptimizing the structure of Figure 18 with the distance from the water proton to the H-bonded bicarbonate oxygen constrained at decreasing distances. Only a shoulder was located in this way at 1.09 Å with energy higher by 5.9 kcal than the water–bicarbonate optimum. At this shoulder, the carbonic acid moiety was bound by 37 kcal and remained in the first shell. We also explored other five-coordinate conformations of the $Zn^{2+}(NH_3)_3OH^{-}H^{+}O_2COH^{-}$ system having different close contacts. No structure lower in energy than the above-mentioned shoulder was found with hydroxyl and carbonic acid. Thus, even in the presence of the metal cation, the formation of the hydroxyl anion and neutral carbonic acid is not apparently energetically favored. Structures in which the protonated bicarbonate oxygen made contact with other protons changed their conformation upon optimization to form other contacts while moving the bicarbonate proton away from the dication.

## Conclusion

The model strongly suggests that when water is bound to zinc the proton transfers from imidazole to formic acid. It is ambiguous

(39) Henkens, R. W.; Merrill, S. P.; Williams, T. J. *Ann. N.Y. Acad. Sci.* **1984**, *429*, 143.

about the position of the hydrogen in the presence of hydroxyl anion. As noted in the Introduction, various interpretations of the state of ionization of the His residues have been advanced with recent data interpreted to reject ionization of a His residue.[15,16] However, this interpretation assumed complete loss of the proton, and this will not happen in the His–Glu couple. The charge density around the proton does not alter much in transferring between His and Glu. In the model calculations with the imidazole and formic acid couple, the Mulliken charge for the shuttling proton is 0.44 when bound to N and 0.45 bound to O irrespective of whether $OH_2$ or $OH^-$ is bound to Zn. The oxygen protonation state induces effects of 0.003 electrons or less. Only a small population shift as a function of the deprotonation of the water is also found for carbon-bound protons and corresponds to the relatively small titration shifts of less than 1 ppm observed for the carbon protons in the histidines.[40-43] Shifts of 5 ppm are not reasonably ascribed to deprotonation of the water proton.

Reinterpretation of the titration shift in an NMR study of H(N) in CoCA[16] provides experimental evidence for the shuttling proton in the Glu–His couple. The intrinsic "diamagnetic" contribution to the shift for the shuttling proton is estimated to be about 5 ppm from the calculated values of the proton shift in histidine[44] and formic acid.[45] For a pH of about 5.0, the proton at −55 ppm is assigned here to be on the Glu. The titration shift[16] of about 5–6 ppm is then attributed mostly to the shift of the proton to His from the Glu as the pH is increased. As noted by Bertini et al.,[16] the main downfield shift is ascribed to large "paramagnetic" dipolar contributions from the Co(II) dication. The deprotonation of the water will also have indirect effects on the charge densities at both metal and hydrogen sites that contribute to the titration curves as seen for the other two histidines. This more complicated assignment of the proton in the His–Glu couple may provide a new way of looking at contradictory interpretations of the NMR data in ZnCA.[40-43] The presence of an anionic residue in the first-shell His–Glu couple would render the CA active site more analogous to the Zn proteases in an electronic as well as a geometric sense.[8]

The effect of such an anionic residue has been calculated to be very large on the electrostatic potential and the binding of anionic first-shell ligands. For isozyme III, the presence of Lys-64, Arg-67, and Arg-91 is considered to alter the local potential sufficiently to shift the $pK_a$ of $EZnH_2O$ below 5.5.[46] These residues would be substantially shielded compared to the His–Glu couple. The binding of the hydroxyl anion to zinc is relatively destabilized by a first-shell anion, which was seen to yield a shift in the proton affinity of 70 kcal from the value with a neutral first shell in this model. The effect on the proton affinity of hydroxyl is still large as the proton shuttles between His and Glu but leaves a negative charge localized near the metal site. The experimental $pK_a$ has to reflect this anionic charge coupled to the first shell of the metal complex. We would suggest that the replacement of the Glu to a Gln would dramatically shift the $pK$ for deprotonation to a smaller value.

The ionicity of the active site should be considered in metal complex mimes. A recent mime for CA found close agreement with the $pK_a$ of bound water[47] but assumes that the macrocyclic triamine is neutral. Although this is certainly true for the crystal structure, the present results suggest that the amine ionizes in solution.

The binding energy of the $CO_2$ substrate is relatively unaffected by changing the ionicity, which suggests that the presence of an anionic protein ligand in the first coordination shell is to enhance the competitiveness of binding of neutral and anionic ligands to the metal cation. When all the His ligands are neutral or the proton is substantially transferred back to His-119, it is more likely that anionic binding at the fourth metal site acts as an inhibitor. The presence of the anionic residue also makes the binding of divalent anions much weaker. For example, the sulfate anion modifies the enzyme behavior through the ionic strength buffer, and the binding to the active site (and not necessarily at the metal) only occurs when another site is protonated.[48]

The small calculated activation energy for the reaction with $CO_2$ agrees with Pullman.[5] As Merz et al.[6] have noted, this step is not the rate-determining step and must be less than the experimental activation energy that is deduced to be less than 10 kcal. The initial binding geometry of $CO_2$ is only slightly distorted as seen in Figure 8. This complex leads directly to reaction, but the $CO_2$ is found to be only slightly perturbed, providing an explanation for the observation of a very slightly shifted vibrational spectra. It differs substantially from that found by Merz et al.,[6] but this could easily arise from internal H bonding to the imidazoles not present in our model and unlikely in the complete enzyme. After reaction produces a stationary point with the bicarbonate proton near the metal, a second stationary point is found with one short Zn–O bond. Again a small activation energy is obtained by the calculated transition state. Except for the relative energetics, this sequence is similar to the results of Jacob et al.[18] However, we have shown that consistent calculations suggest more than one mechanism is available for intramolecular proton transfer. Rapid transfer of labeled oxygen[49] may require both the rotation or rocking of the bicarbonate anion in structure O3[50] and proton transfer between bicarbonate oxygens.[51]

At low pH, the metal will be five-coordinate with two first-shell water molecules, which will not have the same metal to oxygen distances. As the pH is raised and a population of $OH^-$ accumulates, the water is energetically favored in the second shell. The observation of the nearby deep water is rationalized by this. The results are also consistent with the explanation of the hydrogen bonding offered by Eriksson et al.;[30] however, the potential maps do not clearly show that the proton of bound hydroxyl will have a strong enough positive potential to form a favorable electrostatic contact with the oxygen of Thr-199. The substrate also binds in a second shell. Reaction is exothermic with only a slight barrier so this binding complex is productive. The cation does not seriously impede proton transfers for the five-ligand model, and additional waters in the cavity would aid transfer.

The binding energies of bicarbonate anion in four- and five-coordinate complexes are instructive. A single anion has a binding energy of 233 kcal/mol to the +2 complex, but is still bound by 105 kcal/mol in a five-coordinate complex with $OH^-$. The solvation energy is unlikely to exceed 100 kcal, so it raises the question of why bicarbonate is dissociated even after the deprotonation of a coordinated water. There is also strong indication that deprotonation is more difficult in the presence of bicarbonate, suggesting that Thr-199 might carry a positive charge during part of the reaction cycle to aid both deprotonation and removal of bicarbonate from the first shell. When we consider the deprotonation of the His also, however, the binding energy of bicarbonate is reduced to the much smaller value of 19 kcal/mol and ion solvation will dissociate the bicarbonate. A similar line of thought has been presented by Liang and Lipscomb[7] regarding the displacement of bicarbonate except the present calculations find a substantial bicarbonate binding energy even in the presence of the hydroxyl anion. They suggested that the negatively charged Glu-106 reduces the binding energy by about 60 kcal/mol. Without consideration of the screening effects of the hydrogen-bonding chains, it is not possible to quantify the effect of the potentials that are not directly bonded, but it should be noted that,

(40) Campbell, I. D.; Lindskog, S.; White, A. I. *J. Mol. Biol.* **1974**, *90*, 469.
(41) Pesando, J. M.; Grollman, A. P. *Biochemistry* **1975**, *14*, 681.
(42) Pesando, J. M. *Biochemistry* **1975**, *14*, 689.
(43) Gupta, R. K.; Pesando, J. M. *J. Biol. Chem.* **1975**, *250*, 2630.
(44) Prado, F. R.; Giessner-Prettre, C.; Pullman, B. *Org. Magn. Reson.* **1981**, *16*, 103.
(45) Schindler, M.; Kutzelnigg, W. *J. Am. Chem. Soc.* **1983**, *105*, 1360.
(46) Tu, C. K.; Sanyal, G.; Wynns, G. C.; Silverman, D. N. *J. Biol. Chem.* **1983**, *258*, 8867.
(47) Kimura, E.; Shiota, T.; Koike, T.; Shiro, M.; Kodama, M. *J. Am. Chem. Soc.* **1990**, *112*, 5805.
(48) Pocker, Y.; Miao, C. H. *Biochemistry* **1987**, *26*, 8481.
(49) Silverman, D. N.; Tu, C. K. *Biochemistry* **1986**, *25*, 8402.
(50) Lindskog, S.; Engberg, P.; Forsman, C.; Ibrahim, S. A.; Jonsson, B. H.; Simonsson, I.; Tibell, L. *Ann. N.Y. Acad. Sci.* **1984**, *429*, 61.
(51) Liang, J.-Y.; Lipscomb, W. N. *Biochemistry* **1987**, *26*, 5293.

for isozyme III, very strong anion binding is reported.[3] Isozyme III has a much more positive potential in the active site region that would enhance anion binding. The model is so simple that it is easy to suggest that water or other nearby ionic residues or couples such as the Thr–Glu will alter details. It does show the need for the more complete treatment exists and that all of the studies of CA have not properly considered the problem of the ionicity of the metal active site.

**Registry No.** Carbonic anhydrase, 9001-03-0.

# Zeolites versus Aluminosilicate Clusters: The Validity of a Local Description

**G. J. Kramer,*,† A. J. M. de Man,‡ and R. A. van Santen†,‡**

*Contribution from the Koninklijke/Shell-Laboratorium, Amsterdam (Shell Research B.V.), P.O. Box 3003, 1003 AA Amsterdam, The Netherlands, and Laboratory of Inorganic Chemistry and Catalysis, Schuit Institute of Catalysis, Eindhoven University of Technology, P.O. Box 513, 5600 MB Eindhoven, The Netherlands.* *Received December 7, 1990*

**Abstract:** A comparison of force field calculations on extended systems and ab initio quantum chemical calculations on ring structures reveals that the relative energy content of neutral-framework silicas and aluminophosphates is determined by that of the smallest substructures. Energy-minimized structures containing only four, five, and six rings have the same energy content to within 10 kJ/mol. Hypothetical three-ring-containing structures have considerably higher energy content, which may well inhibit their synthesis in the pure $SiO_2$ modification. The results accord with sparse experimental information. Using the same combination of techniques, we demonstrate that substitution of aluminum in silica causes an appreciable, albeit local, distortion of the lattice. The relaxation energy for such a substitution amounts to 100–200 kJ/mol, depending on the way charge compensation is accomplished.

## 1. Introduction

Secondary building units (SBU) play an important role in the structural study of zeolites and aluminophosphates. The SBUs are small composite entities like rings or double rings, built from corner sharing $TO_4$ (T = Si, Al, P) tetrahedrons, which can be used to formally describe the framework topology.[1] Thus, they provide a useful tool for classifying the large number of known zeolite networks as well as for systematically enumerating the endless number of hypothetical four-connected networks.[2-4] At a less abstract level, their proven existence in silica synthesis gels[5,6] has led to speculations concerning their role in steering the still poorly understood process of zeolite synthesis.[7-10]

Lastly, SBUs are very similar to the clusters that are used by theoretical chemists as model systems for zeolites, in studies on zeolite stability,[11] acidity,[12,13] water coordination,[14] and framework substitutions.[15-17] The use of ab initio quantum chemical calculations on these small clusters contrasts with the other approach of zeolite theoretical chemistry: the classical modeling of extended systems, using force fields to describe the interactomic interactions.[18,19] So far it has been difficult to reconcile the two theoretical approaches.

Force field methods are suited to deal with extended structures built from large unit cells. However, since they are based on effective, classical potentials, they are not able to handle electronic effects that control the chemical reactivity of isomorphously substituted zeolites. The theoretical study of the acidity of protons attached to a zeolite lattice provides an example of such a problem. This kind of subject can at present only be approached by application of quantum chemical calculus to small clusters. The variational character of the ab initio SCF scheme of quantum chemistry implies that the results are unambiguous only for geometry-optimized clusters.[20] The question that emerges is whether or not, or to what extent, the results on geometry-optimized (free) clusters still have any bearing on the chemically reactive sites embedded in extended systems (zeolites), where the geometric freedom of the cluster is restricted.

In this paper, we will explore the extent to which zeolitic substructures can still be considered free building blocks, when embedded in the extended zeolite. To this end, we employ both ab initio quantum chemical tools and force field methods. The force field that will be used is based on the parametrization of

† Koninklijke/Shell-Laboratorium, Amsterdam.
‡ Eindhoven University of Technology.

(1) Meier, W. M.; Olsen, D. H. *Atlas of Zeolite Structure Types*, 2nd revised ed.; Butterworth: Cambridge, 1987.
(2) Barrer, R. M. *Zeolite and Clay Minerals as Sorbents and Molecular Sieves*; Academic Press: London, 1978.
(3) Smith, J. V. *Am. Mineral.* **1977**, *62*, 703–709. *Ibid.* **1978**, *63*, 960–969. *Ibid.* **1979**, *64*, 551–562.
(4) Meier, W. M. In *New Developments in Zeolite Science and Technology*; Murakumi, Y., et al., Eds.; Studies in Surface Science and Catalysis 28; Elsevier: Amsterdam, 1986; pp 13–22.
(5) Groenen, E. J. J.; Kortbeek, A. G. T. G.; Mackay, M.; Sudmeijer, O. *Zeolites* **1986**, *6*, 403.
(6) Kinrade, S. D.; Swaddle, T. W. *Inorg. Chem.* **1988**, *27*, 4253–4259.
(7) Van Santen, R. A.; Keijsper, J.; Ooms, G.; Kortbeek, A. G. T. G. In *New Developments in Zeolite Science and Technology*; Murakumi, Y., et al., Eds.; Studies in Surface Science and Catalysis 28; Elsevier: Amsterdam, 1986; pp 169–175.
(8) Szostak, R. *Molecular Sieves, Principles of Synthesis and Identification*; Van Nostrand Reinhold: New York, 1989; see also references therein.
(9) Dent-Glasser, L. S.; Lachowski, E. E. *J. Chem. Soc., Dalton Trans.* **1980**, 399.
(10) Knight, C. T. G. *Zeolites* **1990**, *10*, 140–144 and references therein.
(11) Van Beest, B. W. H.; Verbeek, J.; Van Santen, R. A. *Catal. Lett.* **1988**, *1*, 147–154.
(12) Sauer, J.; Kölmel, C. M.; Hill, J. R.; Ahlrichs, R. *Chem. Phys. Lett.* **1990**, *164*, 193–198.
(13) Beran, S. *J. Phys. Chem.* **1990**, *94*, 335–337.
(14) Sauer, J.; Horn, H.; Häser, M.; Ahlrichs, R. *Chem. Phys. Lett.* **1990**, *173*, 26–32.
(15) Fripiat, J. G.; Galet, P.; Delhalle, J.; Andrè, J. M.; Nagy, J. B.; Derouane, E. G. *J. Phys. Chem.* **1985**, *89*, 1932–1937.
(16) Derouane, E. G.; Fripiat, J. G. *Zeolites* **1985**, *5*, 165–172.
(17) O'Malley, P. J.; Dwyer, J. *Zeolites* **1988**, *8*, 317–321.
(18) Van Santen, R. A.; Ooms, G.; Den Ouden, C. J. J.; Van Beest, B. W. H.; Post, M. F. M. *Zeolite Synthesis*; ACS Symposium Series 398; American Chemical Society: Washington, DC, 1989; pp 617–633.
(19) Jackson, R. A.; Catlow, R. C. A. *Mol. Simul.* **1988**, *1*, 207–224.
(20) Hehre, W. J.; Radom, L.; Schleyer, P. v. R.; Pople, J. A. *Ab Initio Molecular Orbital Theory*; John Wiley & Sons: New York, 1986; p 92.

0002-7863/91/1513-6435$02.50/0 